RSC Advances

This is an *Accepted Manuscript*, which has been through the Royal Society of Chemistry peer review process and has been accepted for publication.

Accepted Manuscripts are published online shortly after acceptance, before technical editing, formatting and proof reading. Using this free service, authors can make their results available to the community, in citable form, before we publish the edited article. This *Accepted Manuscript* will be replaced by the edited, formatted and paginated article as soon as this is available.

You can find more information about *Accepted Manuscripts* in the Information for Authors.

Please note that technical editing may introduce minor changes to the text and/or graphics, which may alter content. The journal's standard Terms & Conditions and the Ethical guidelines still apply. In no event shall the Royal Society of Chemistry be held responsible for any errors or omissions in this *Accepted Manuscript* or any consequences arising from the use of any information it contains.

ROYAL SOCIETY OF CHEMISTRY

www.rsc.org/advances

Nitrogen Mediated Electronic Structure of Ti(0001) Surface

Lei Li[a], Fan-Ling Meng[a], Xiao-Ying Hu[b], Liang Qiao[b], Chang Q Sun,[c] Hong-Wei Tian [a]*, and Wei-Tao Zheng[a*]

[a] Department of Materials Science and Key Laboratory of Automobile Materials of MOE and State Key Laboratory of Superhard Materials, Jilin University, Changchun 130012, China.

[b] College of Science, Changchun University, Changchun 130022, China

[c] School of Electrical and Electronic Engineering, Nanyang Technological University, Singapore 639798.

*Corresponding author, *E-mail: Tianhw@jlu.edu.cn; wtzheng@jlu.edu.cn*

RSC Advances Accepted Manuscript

Abstract

The unusual ability of nitrogen in functionalizing transition metals has tremendous implications to the nitride compounds for chemical, electronic, optical, mechanical, and tribological applications yet a consistent insight into the underneath mechanism remains yet a challenge. A combination of the density function theory and photoelectron spectroscopy revealed that the nitrogen atom prefers the tetrahedron bonding geometry in the Ti(0001) skin, which derives four additional valence density-of-states: the bonding electron pairs, nonbonding lone pairs, electronic holes, and antibonding dipoles. Dipole formation modulates the work function, electron–hole generation opens the bandgap, nonbonding interaction ensures the superlubricity of the N-Ti(0001) skin.

Keywords: Ti(0001); Nitrogen; DFT; Entrapment; Polarization, UPS

RSC Advances Accepted Manuscript

1 Introduction

Nitride compounds have formed a class of materials with fascinating properties that have widely been used for mechanical and elastic enhancement, wear and corrosion resistant, magnetic modulation, and photon and electron emission such as GaN light emission devices, etc. [1-7]. Even though the performance of nitrides has been intensively investigated and widely used, understanding the correlation between the local atomic-bonding, the energy band structures, and the observed, or predicted properties of such compounds and their interdependence is still in its infancy. Concerns about the correlation between the chemical bond and valence density of states (DOS) and their effects on materials performance are therefore necessary.

Adsorption of nitrogen on the Ti(0001) skin has been investigated by several experiment and theoretical studies [8-15]. By low energy electron diffraction (LEED) and Auger electron spectroscopy (AES) measurements, Shih et al. [10] suggested that the nitrogen exposure creates a Ti(0001)-(1×1)-N phase followed by a Ti(0001)-($\sqrt{3} \times \sqrt{3}$)-N structure, in which nitrogen atoms occupy octahedral holes between the first and second metal layers firstly. They also indicated that three outermost layers of the Ti(0001)-(1×1)-N surface have a structure essentially identical to those of TiN(111). Fukuda et al. [12] has been experimentally investigated that the effect of nitrogen is very similar to that of oxygen, the work function decreases slightly at lower exposures of N_2, then reverses and undergoes a substantial increase at saturation exposures. It is generally accepted that the initial negative change in the work function is due to the N_2 molecules dissociate and occupy initially sites just below the first metal atomic layer which induced the negative polarization of the adsorbate pointed inward [16]. However, it is contradictory that oxygen atoms tend to absorb above the Ti(0001) surface and nitrogen atoms tend to absorb below the surface in the initial stage [17, 18].

In the present study, we report density functional theory (DFT) revelation of four DOS features in the valence band of the Ti(0001) surface, representing the bonding electron pairs, nonbonding lone pairs, metal electronic holes, and metal antibonding dipoles. The polarization of the conduction electrons by the nonbonding states lowers the work function of the Ti(0001) skin upon nitrogen adsorption.

RSC Advances Accepted Manuscript

The generation of the electronic holes turns the conductor into semiconductor.

2. DFT calculations

We conducted spin-polarized DFT calculations using the CASTEP code [19] with ultrasoft pseudo-potentials, and a kinetic energy cutoff of 400 eV. The exchange correlation function was formulated using the generalized gradient approximation (GGA) with the Perdew–Wang parameterization (known as GGA-PW91) [20], which have proved to be more reasonable than other functional [21]. The structural optimization was performed until the energy change per atom was less than 5×10^{-7} eV/atom, the forces on atoms were less than 0.01 eV/Å, all the stress components were less than 0.02 GPa and a maximum displacement of 5×10^{-4} Å was reached.

The hcp-structured single crystal Ti structure yields a lattice constant of a = 2.935 Å, c = 4.640 Å, which gives c/a = 1.581. These calculated values are consistent with the experiment values of a = 2.949 Å, c = 4.677 Å and c/a = 1.586 [22], and in good agreement with previous DFT results [16, 23].

To optimize the computational cost and the accuracy of the DFT calculations, a six-layer slab of the Ti(0001) surface with a vacuum region of 20 Å is simulated as three-dimensional infinite periodic structures by defining a supercell and periodic boundary conditions in all three principal axes. The bottom two layers were fixed at their bulk truncated structure. A dipole correction was applied to avoid slab-slab interactions [24].

3 Results and analysis

With respect to observations, we assumed that nitrogen adsorbs to the Ti(0001) skin in a mixed monolayer and multilayer configuration. According to LEED and AES measurements, an initial (1×1) monolayer and subsequent (1×1) + ($\sqrt{3} \times \sqrt{3}$) pattern multilayer can rationalize the subsequent DFT calculations. To calculate the monolayer and multilayer surface structures, two surface models, i.e.,

RSC Advances Accepted Manuscript

(2×2) and (3×3) supercell as shown in Figure 1(a), are used in this study with a corresponding k-mesh of 6 × 6 × 1 and 4 × 4 × 1, respectively. The calculated work function of clean surface is 4.47 eV that is consistent with experimental values (4.45–4.60 eV) [17] and previous DFT calculations (4.45±0.01 eV) [13, 25].

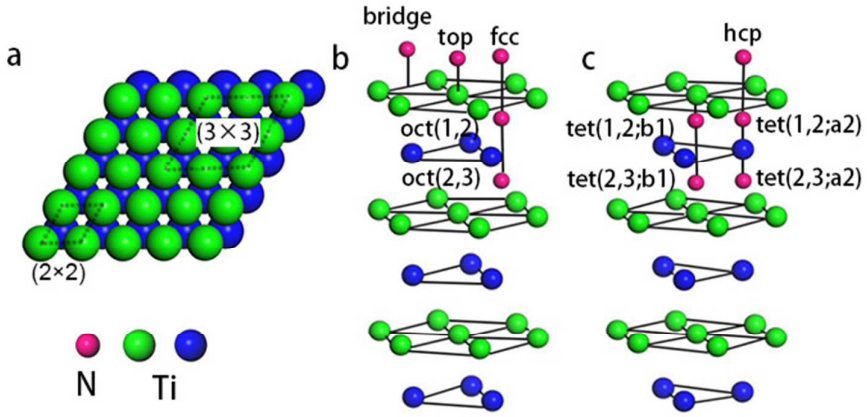

Figure 1 (a) The top view of the Ti(0001) surface with indication of the (2 × 2) and (3 × 3) unit cells. Perspective views (b, c) of N adsorption sites. The symbol oct(*i,j*) denotes the octahedral sites between the *i* th and $i+1$ th layers, and tet(*i,*:a*j*(or b*i*)) means the tetrahedral site located directly below the *i* th layer.

3.1 Adsorption sites and N-Ti bond lengths

Figure 1b and c shows the possible chemisorption sites. A series of repeated optimization results in the average adsorption energy of nitrogen atoms and work function for possible adsorption sites, as summarized in Table 1.

The following formulates the adsorption energy:

$$E_{ads} = \frac{1}{n}\left(E_{clean} + \frac{n}{2}E_{N_2} - E_{N/Ti(0001)}\right);$$

where *n* is the number of nitrogen atoms in the unit cell, $E_{N/Ti(0001)}$, E_{clean} and E_{N_2} represent the total

RSC Advances Accepted Manuscript

energies per unit cell of the nitrogen-adsorbed Ti slab, the clean Ti slab, and the N_2 molecule, respectively.

Table 1 Average adsorption energy per N atom at various adsorption sites of Ti(0001) skin and the derived work function. The work function of the clean Ti(0001) surface is 4.47 eV

Adsorption concentration (ML)	**Adsorption site**	**Adsorption Energy (eV)**	**Work function (eV)**
0.25ML	fcc	3.46	4.39
	hcp	3.42	4.54
	bridge	-	-
	top	-	-
	oct (1,2)	3.97	4.21
	tet (1,2; b1)	2.73	4.025
	tet (1,2; a2)	-	-
	oct(2,3)	4.52	4.267
0.50ML	fcc	3.12	5.06
	oct(1,2)	3.82	4.13
	fcc+ oct(1,2)	3.68	4.75
	hcp+ oct(1,2)	3.80	4.68
0.75ML	fcc	2.94	5.49
	oct(1,2)	4.13	4.20
	fcc+ oct(1,2)	3.82	4.73
	hcp+ oct(1,2)	3.89	4.46
1.00ML	fcc	2.84	6.11

RSC Advances Accepted Manuscript

	oct(1,2)	4.16	4.55
	fcc+ oct(1,2)	3.88	4.22
	hcp+ oct(1,2)	3.94	4.94
1.33ML	oct(1,2)+fcc	3.73	4.93
	oct(1,2)+hcp	3.90	4.88

The results in Table 1 indicate the following.

First, in the initial stages of adsorption, i.e., at 0.25 ML coverage, the subsurface octahedral (oct(1,2)) site was found to be the most stable location for atomic nitrogen to reside in the Ti(0001) skin. The fcc sites is slightly favorable than the hcp sites, while the top, bridge and tetrahedral sites are energetically unfavorable. Then, nitrogen cover full oct(1,2) sites and form a stable (1×1) structure with a saturation coverage 1.00 ML.

Second, with nitrogen concentration increasing, additional $(\sqrt{3} \times \sqrt{3})$ structure formed on the top surface. Due to the interaction of N atoms in adjacent interlayer, the $(\sqrt{3} \times \sqrt{3})$ surface structure tend to occupied hcp sites.

Third, the work function changes ($\Delta\Phi$) relation to the Ti(0001) surface are shown in Figure 2 and Table 1. We have used as reference the calculation work function of clean Ti(0001) surface (4.47 eV). The work function with a initially decrease, then reverses and undergoes a substantial increase at saturation exposures, which are in excellent agreement with experimental observations [12].

RSC Advances Accepted Manuscript

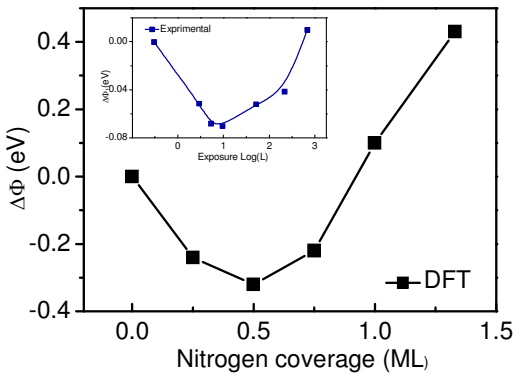

Figure 2 Coverage dependence of the work function for the Ti(0001)-N surface, compared with experimental observations (the inset) [12].

Table 2 Relaxation of the Ti(0001) interlayer spacing and the average Ti-N bond length. The bulk interlayer space is 2.32 Å.

	Relaxation (%)			Bond length (Å)		
	ΔD_{12}	ΔD_{23}	ΔD_{34}	d_N	$d_{Ti(1)-N}$	$d_{Ti(2)-N}$
Ti(0001) (present)	-6.9	+2.9	-1.1	-		
Experiment [22]	-2.1			-		
DFT [26]	-6.8	+2.8	-0.5	-		
Ti(0001)-(1×1)-N						
0.25 ML	+0.8	+0.1	-0.4	-	2.034	2.047
0.50 ML	+3.1	+0.5	+1.2	-	2.050	2.056
0.75 ML	+2.0	+6.3	-1.3	-	2.052	2.072
1.00 ML	+2.0	+4.6	-0.8	-	2.060	2.073
Ti(0001)-(1×1)($\sqrt{3}\times\sqrt{3}$)-N						
1.33 ML	+7.3	+0.6	-1.6	1.932	2.087	2.085
Bulk TiN(111)					2.123	1.227

Table 2 lists the relaxation of the Ti(0001) slab and the N–Ti bond length of the N–Ti(0001) skin.

RSC Advances Accepted Manuscript

The relaxation ΔD_{ij} is defined by the change in interlayer spacing between the *i*th and *j*th Ti metal layers. The d_N indicates the average bond length of surface nitrogen atoms (hcp) with respect to topmost Ti plane. The $d_{Ti(1)-N}$ and $d_{Ti(2)-N}$ indicate the average bond length of subsurface nitrogen atoms (Oct(1,2)) with respect to topmost Ti plane and second plane, respectively.

For clean Ti(0001) skin, our calculations yield a contraction of the topmost interlayer spacing of -6.9%, while the second and third interlayer spacing expand and contract by +2.9% and -1.1%, respectively. The contraction of the topmost interlayer spacing is in good agreement with another DFT calculations (-6.8%), while LEED analysis of the Ti(0001) surface predicts a contraction of only -2.1% [22], significantly less than predicted theoretically. The error is due to the main relaxation occurring on the z direction of slab in DFT calculation. When N atoms going into subsurface interlayer, the relaxation induced by undercoordination of skin occurs obviously decreased. However, the surface N atoms significantly expand the topmost interlayer.

For subsurface adsorption, the N-Ti average bond length gradually increased with nitrogen coverage. The Ti(0001)-(1×1)-N phase is essentially identical to one (111) double-layer of TiN crystal.

3.2 Valence density of states

3.2.1 Monolayer adsorption

Figure 3a shows the coverage dependence of the valence DOS for the N-Ti(0001) skin at the Oct(1,2) adsorption sites with different coverages calculated by (2×2) model. N adsorption does not simply add its 2s and 2p states to the valence bands of Ti(0001) but exchanges and polarizes electrons of the pure Ti. Compared with the clean Ti(0001) skin (Figure 4a), nitrogen adsorption creates obvious DOS features at +2.0 eV (antibonding), ~ 0 eV (nonbonding), -2.0 to +1.0 eV (holes) and -4.0 to -7.0 eV (bonding), which are surprisingly consistent with the results from O-Ti(0001) skin (Figure 4b).

The DOS features between -4.0 and -7.0 eV are derivatives of the Ti-N bonds that are stronger than the original pure Ti-Ti bonds. The stronger interaction lowers the system energy and stabilizes the system. It is reason that TiN is metal ceramic material with high hardness, excellent chemical and thermal stability, reliable mechanical performance at high temperatures. The antibond states (+2.0 eV)

RSC Advances Accepted Manuscript

arise from polarization of the Ti 3d electronics by the lone pairs of nitrogen. Deeply moving of bonding states and shallow moving of antibonding states lead to form holes near the Fermi level.

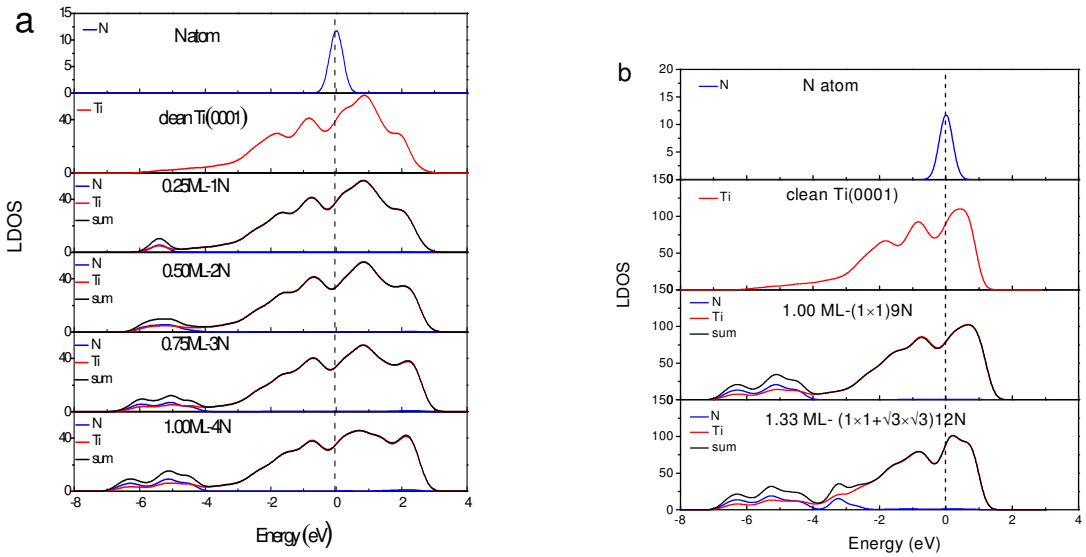

Figure 3 Ti(0001)-N coverage dependence of the valence local density-of-states (LDOS). (a) Monolayer adsorption that N occupied at oct(1,2) sites simulated by (2×2) model. (b) Multilayer adsorption for the Ti(0001)-(1×1)-9N and $(1\times1)(\sqrt{3}\times\sqrt{3})$-12N simulated by (3×3) model. Blue and red lines represent the LDOS of N and Ti components, respectively. Black line are the sum of all these. E = 0 is the referential Fermi level.

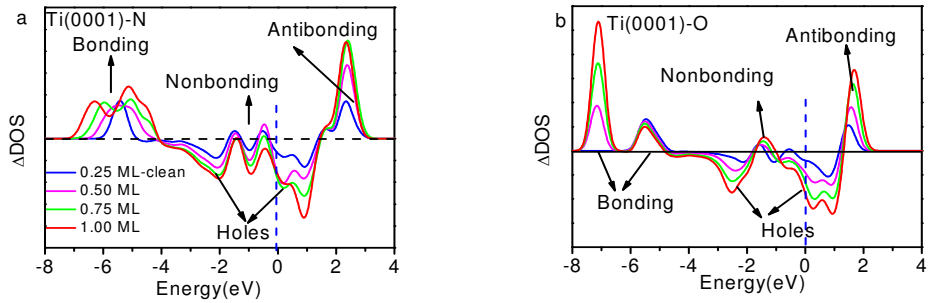

Figure 4 Coverage dependence of the ZPS of n(Ti + X)-n(Ti) for (a) x-N and (b) x = O with respect to that of clean Ti(0001) surface [18]. Both sets of profiles exhibit four DOS features that correspond to antibonding dipoles, nonbonding, bonding states and holes. E = 0 eV is the referential Fermi energy.

RSC Advances Accepted Manuscript

3.2.2 Multilayer adsorption

For high nitrogen coverage, multilayer adsorption model, i.e., Ti(0001)-(1×1)($\sqrt{3} \times \sqrt{3}$)-N structure is formed based on Ti(0001)-(1×1)-N phase, modeled by (3×3) supercell. Figure 3b shows the corresponding valence LDOS. Compared with the clean Ti(0001) skin (Figure 5), similar four valence DOS features appeared: antibonding (~ +1.5 eV), nonbonding (~ 0 eV), holes (-3 to 1 eV) and bonding (-4 eV and -6 eV) states. However, a new bonding state appears at ~ -3.0 eV, which could consider is H-like bonding (N^{-3} - $Ti^{+/dipole}$: N^{-3}). Meanwhile, antibonding states move to the deeply energy-level and intensity decreased significantly, it is due to H-like bond forms annihilating the electron cloud of the dipoles to the bonding orbitals of the nitrogen at hcp sites.

Figure 5 inset shows the differential UPS spectra for Ti(0001) surface with nitrogen exposures based on the zone-resolved photoelectron spectroscopy (ZPS) technique [27]. We collected the UPS data of Ti(0001) surface before and after N adsorption [8]. Upon the spectral peak area normalization and background correction, we then differentiated the spectra to get the atomic-scale, zone-selective information of the bonding and electronic dynamics. The ZPS features below E_F confirms the presence of the mixed hole-nonbonding features as the spectral valley near the E_F and the bonding attributes at -7.0 to -4.0 eV as a peak.

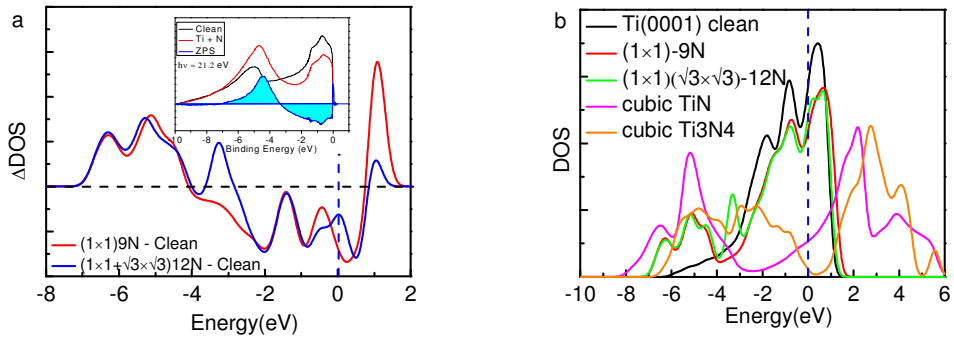

Figure 5 (a) Comparison of the measured (inset) [8] and calculated ZPS profiles of n(Ti + N)-n(Ti), at Ti(0001)-(1×1)-9N and Ti(0001)-(1×1)($\sqrt{3} \times \sqrt{3}$)-12N with respect to that of clean Ti(0001) surface. (b) The valence DOS dependence on the ration of nitrogen and titanium. Cubic Ti_3N_4

RSC Advances Accepted Manuscript

presents a 0.219 eV bandgap.

3.3 Band gap creation and work function evolution

Figure 5b shows the sharp fall of the DOS features near the E_F results from the holes production in the process of nitrogen ratio increase gradually, until Ti_3N_4 crystal opening a 0.219 eV bandgap. The sake of simplicity, both TiN and Ti_3N_4 are cubic-type structure selected in our calculation. The bandgap value of cubic Ti_3N_4 is slightly small than the theoretical prediction from Peter [28], due to different calculation method. This mechanism may provide reference for band gap modulation of titanium nitride.

Figure 4a and Figure 5a show the antibonding states move to shallow level at low nitrogen coverage and move deeply when the coverage increases. This finding could explain the change of work function. The change of work function corresponds to the shift of the antibonding dipole states, which provides information about the dipoles formation and H-like bond formation. Dipole formation can deepen the antibonding states and reduces the work function; H-like bond formation can shallow the antibonding sub-band and restores the work function, which stabilizes the entire system. According to above, the work function or the threshold in cold cathode field emission of nitrogen compounds can be modulated by the nitrogen content and sites.

4. Discussion

We confirm that the bond-band correlation of nitrides consistent with the bond–band–barrier (3B) correlation notation predictions [29]: C, N, O, and F can interact with arbitrary metal to form a tetrahedron with four additional DOS features, i.e., the bonding electron pairs, nonbonding lone pairs, metal electronic holes, and metal antibonding dipoles, which dominate the performance of compounds.

The 3B correlation notation indicates that the sp^3-orbital hybridization is necessary for O, N, C, and F interacting with atoms in the solid phase to form quasi-tetrahedron like H_2O, NH_3, CH_4, and FH, which determines the crystallography, morphology, band structure, and the chemical physical

RSC Advances Accepted Manuscript

properties of the chemisorbed skins. Figure 6 (a) illustrates the physical model of a nitride (NB_4) quasi-tetrahedron obtained by replacing the hydrogen in the NH_3 molecule with atoms of arbitrary electropositive element B.

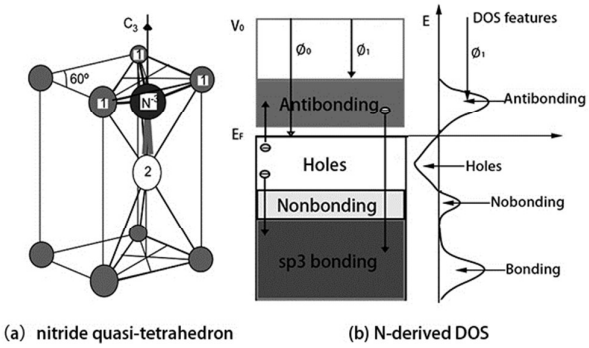

Figure 6 (a) NB_4 nitride quasi-tetrahedron structure and (b) the associated valence DOS features. Smaller ions (labeled 1) donate electrons to the central N acceptor of which the sp orbital hybridizes with production of a nonbonding lone pair. N hybridizes its sp-orbit and interacts with arbitrary element B (1 and 2) through bonding (1-N) and nonbonding lone pair (2-N) to form the quasi-tetrahedron: $NB_4 = N^{3-} + 3B^{+}$ (labeled 1) + B^{dipole} (labeled 2). Arrow represent the process of charge transportation giving rise to four DOS features [29].

Upon interacting with atoms B in a solid phase, the sp orbital of the N atom hybridizes essentially into four directional orbitals, which similar to O atom. There of the four hybridized orbits are occupied by shared electron pairs. The remaining one is occupied by the lone electron pair of nitrogen, which entitles a nitrogen quasi-tetrahedron of C_{3v} group symmetry. Because of the NB_4 tetrahedron formation, the electronic structure of the B host solid is modified with four additional valence DOS features: bonding ($< E_F$), nonbonding ($\sim E_F$), holes ($\sim E_F$), and antibonding ($> E_F$) states. This nitridation defines four features to the valence band of the chemisorbed system in the following electronic dynamics (see Figure 6(b)):

(i) Nitrogen catches electrons from its neighboring B atoms to N-B bond and fill its $2s^2p^4$ orbits, which produces energy states slightly lower than the 2p-level of the nitrogen, therefore, electrons in the bonding states should be more stable compared with the otherwise electrons in the host structures. This may explain why a nitride surface is corrosion resistant.

(ii) The N-B bond formation also creates electron holes leave behind the B^{+} ion, the holes are produced below the E_F and hence causing the formation of a bandgap.

RSC Advances Accepted Manuscript

(iii) The sp^3-orbit hybridization takes place, which creates the nonbonding lone pair states just below the Fermi level (E_F)

(iv) The lone pair polarizes its neighboring atoms to form the pinned dipoles (B^{dipole}) that fill the antibonding orbits. The dipoles reduces the work function from Φ_0 to Φ_1. So, doping proper amount of nitrogen can lower the work function or threshold in cold-cathode field emitters.

(v) Overdosing nitrogen in chemisorption, the overdosed nitrogen gets electrons from the dipoles that are polarized into antibonding states, H-like bond network (N^{-3} - $B^{+/dipole}$: N^{-3}) forms at the skin, which annihilates the skin dipoles and raises the work function. The '-' and ':' represent the bonding pair and the nonbonding lone pair, respectively. The arrow from the antibonding to bonding states corresponds to the process of H-like bond formation.

5 Conclusions

Consistency in the 3B theory expectation, DFT calculations, and UPS measurement clarified the essentiality of tetrahedron formation of N–Ti with four additional DOS features: bonding electron pairs; nonbonding lone pairs; holes; and antibonding dipoles. These DOS features determine the physical properties of the chemisorbed Ti(0001) surface. Ti–N bonding states lower the system energy and passivate the Ti(0001) surface; nonbonding lone pairs and antibonding dipoles modify the work function that changes with adsorption concentration and adsorption sites of nitrogen. Creation of electron holes gradually opens the bandgap turning metallic Ti into Ti_3N_4 semiconductor. The findings is consistent with oxygen adsorption on Ti(0001) skin. Observations will be helpful for understanding the unusual behavior of nitrides and provide powerful means for designing and fabricating functional materials.

Acknowledgement

Financial support from the NSF (No. 51472106) of China and the NSF (No. 20140101107JC) of Jilin Province are highly appreciated. The DFT calculations utilized resources at the High Performance Computing Center of Jilin University, China.

1. Waltereit, P., et al., *Nitride semiconductors free of electrostatic fields for efficient white light-emitting diodes.*

RSC Advances Accepted Manuscript

Nature, 2000. **406**(6798): p. 865-868.
2. P, S., *Laser nitriding of metals.* Progress in Material Science, 2002. **47**(1): p. 1-161.
3. Gu, Z., et al., *On the nature of point defect and its effect on electronic structure of rocksalt hafnium nitride films.* Acta Materialia, 2014. **81**: p. 315-325.
4. Wang, S., et al., *The Hardest Superconducting Metal Nitride.* Scientific Reports, 2015. **5**: p. 13733.
5. Patsalas, P., N. Kalfagiannis, and S. Kassavetis, *Optical Properties and Plasmonic Performance of Titanium Nitride.* Materials, 2015. **8**(6): p. 3128-3154.
6. Morkoç, H. and S.N. Mohammad, *High-Luminosity Blue and Blue-Green Gallium Nitride Light-Emitting Diodes.* Science, 1995. **267**(5194): p. 51-55.
7. Yang, G.M., et al., *Density Functional Theory Calculations for the Quantum Capacitance Performance of Graphene-Based Electrode Material.* The Journal of Physical Chemistry C, 2015. **119**(12): p. 6464-6470.
8. Eastman, D.E., *Photoemission energy level measurements of sorbed gases on titanium.* Solid State Communications, 1972. **10**: p. 933-935.
9. SHIH, H.D. and F. JONA, *Atomic underlayer formation during the reaction of Ti {0001} with nitrogen.* Surface Science 1976. **60**: p. 445-465.
10. Shih, H., et al., *Low-Energy-Electron-Diffraction Determination of the Atomic Arrangement in a Monatomic Underlayer of Nitrogen on Ti(0001).* Physical Review Letters, 1976. **36**(14): p. 798-801.
11. Brearley, W. and N.A. Surplice, *Changes in the work function of titanium films owing tothe chemisorption of N_2, O_2, CO and CO_2.* Surface Science, 1977. **64**: p. 372-374.
12. Fukuda, Y., W.T. Elam, and R.L. Park, *Nitrogen, Oxygen, and Carbon Monoxide Chemisorption on Polycrystalline Titanium Surfaces.* Applied Surface Science, 1978. **1**: p. 278-287.
13. Feibelman, P. and F. Himpsel, *Spectroscopy of a surface of known geometry: Ti(0001)-N(1×1).* Physical Review B, 1980. **21**(4): p. 1394-1399.
14. BIWER, B.M. and S.L. BERNASEK, *A photoelectron and energy-loss spectroscopy study of Ti and its interaction with H_2, O_2, N_2 and NH_3.* Surface Science, 1986. **167**: p. 207-230.
15. M.V.Kuznetsov and E.V.Shalaeva, *Competing Adsorption of Nitrogen and Oxygen at the Ti(0001) Face : XPS Examination.* The Physics of Metals and Metallography, 2004. **97**: p. 485-494.
16. Liu, S.-Y., et al., *Ab initio study of oxygen adsorption on the Ti(0001) surface.* J. Phys. Condens. Matter, 2007. **19**(22): p. 226004.
17. Hanson, D., R. Stockbauer, and T. Madey, *Photon-stimulated desorption and other spectroscopic studies of the interaction of oxygen with a titanium (001) surface.* Physical Review B, 1981. **24**(10): p. 5513-5521.
18. Li, L., et al., *Oxygenation mediating the valence density-of-states and work function of Ti(0001) skin.* Phys. Chem. Chem. Phys., 2015. **17**(15): p. 9867-9872.
19. Hoffmann, M.R., et al., *Environmental applications of semiconductor photocatalysis.* Chemical Reviews, 1995. **95**: p. 69-96.
20. Perdew, J., P. Ziesche, and H. Eschrig, *Chapter Unified Theory of Exchange and Correlation Beyond the Local Density Approximation*. Electronic Structure of Solids, ed. P. Ziesche and H. Eschrig, Akademie, Berlin. 1991.
21. Guo, J., et al., *Study of hydrogen adsorption on the Ti (0001)-(1×1) surface by density functional theory.* Applied Surface Science, 2008. **255**(5): p. 3164-3169.
22. Shih, H.D., et al., *The structure of the clean Ti(0001) surface.* J. Phys. C: Solid State Phys., 1976. **9**: p. 1405-1416.
23. Feibelman, P.J., J.A. Appelbaum, and D.R. Hamann, *Electronic structure of a Ti(0001) film.* Physical Review B, 1979. **20**: p. 1433.
24. Bengtsson, L., *Dipole correction for surface supercell calculations.* Physical Review B, 1991. **59**: p. 12301.
25. Huda, M. and L. Kleinman, *Density functional calculations of the influence of hydrogen adsorption on the*

RSC Advances Accepted Manuscript

surface relaxation of Ti (0001). Physical Review B, 2005. **71**(24): p. 241406.

26. Da Silva, J.L.F., C. Stampfl, and M. Scheffler, *Converged properties of clean metal surfaces by all-electron first-principles calculations.* Surface Science, 2006. **600**(3): p. 703-715.
27. Liu, X., et al., *Coordination-Resolved Electron Spectrometrics.* Chemical Reviews, 2015. **115**(14): p. 6746-810.
28. Kroll, P., *Hafnium Nitride with Thorium Phosphide Structure: Physical Properties and an Assessment of the Hf-N, Zr-N, and Ti-N Phase Diagrams at High Pressures and Temperatures.* Physical Review Letters, 2003. **90**(12): p. 125501.
29. Sun, C.Q., *Relaxation of the Chemical Bond*. Springer Series in Chemical Physics 108. Vol. 108. 2014 Heidelberg: Springer. 807 pp.

RSC Advances Accepted Manuscript

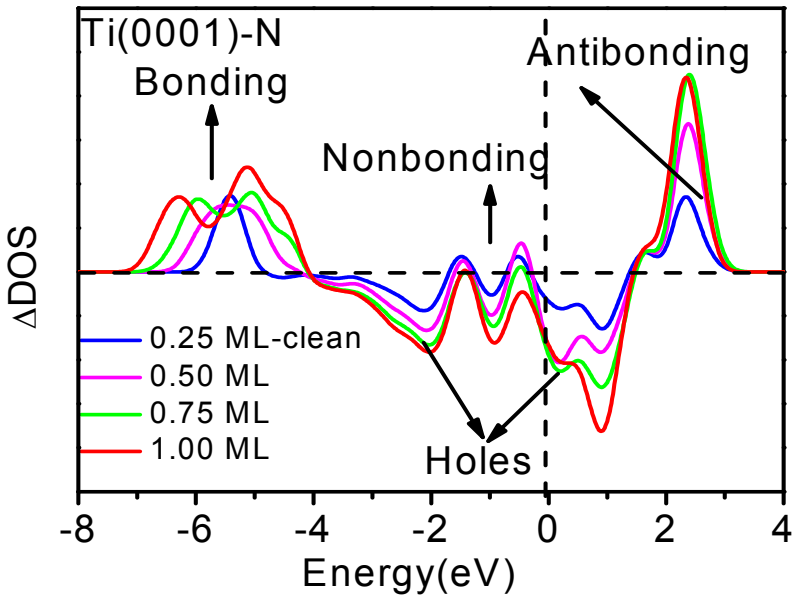

The unusual ability of nitrogen in functionalizing transition metals has tremendous implications to the nitride compounds for chemical, electronic, optical, mechanical, and tribological applications yet a consistent insight into the underneath mechanism remains yet a challenge. A combination of the density function theory and photoelectron spectroscopy revealed that the nitrogen atom prefers the tetrahedron bonding geometry in the Ti(0001) skin, which derives four additional valence density-of-states: the bonding electron pairs, nonbonding lone pairs, electronic holes, and antibonding dipoles. Dipole formation modulates the work function, electron–hole generation opens the bandgap, nonbonding interaction ensures the superlubricity of the N-Ti(0001) skin.

RSC Advances Accepted Manuscript